Applied FEM Techniques in Ceramic Feedthru Package Design

Mark D. Eblen
Kyocera America, Inc.
Research & Development
San Diego, CA
Phone: 858/614-2537
email: mark.eblen@kyocera.com

Abstract

With the advent of high power GaAs MMIC devices, hermetic feedthru microelectronic packages have become increasingly more important in aerospace applications. Critical to the design of this product, is the thermal expansion mismatch that takes place during brazing between package components. This thermal expansion mismatch produces high residual stresses in the alumina feedthru that, depending on the severity, can lead to premature component failure. In the present work, ANSYS™ finite element method software has been coupled with CARES/Life failure probability design software to quantitatively determine the reliability of this package.

1.0 Introduction

With the advent of high power GaAs MMIC devices, hermetic ceramic feedthru packages have become increasingly more important in aerospace applications. Critical to the robust design of this product, is the thermal expansion mismatch that takes place during brazing between the alumina feedthru and other package level components. This general expansion mismatch produces residual thermal strain in the feedthru, which depending on the severity, can lead to hermetic failure under harsh field conditions signaling premature systems failure. While hermeticity loss would not cause immediate failure of the device, gradual moisture ingress will certainly degrade the electrical performance of the semiconductor components inside the lid sealed package [1].

In the present work, the finite element method (FEM) software program ANSYS™ has been utilized as a convenient tool for investigating the design choices that minimize this effect. However, as with any computational tool, proper implementation of the methodology must address a host of technical challenges such as:

- Temperature dependent material property characterization.
- Modeling assumptions such as isothermal behavior and stress relaxation.
- Fine detail stress analysis resolution.
- Statistical nature of failure in brittle materials.
- Experimental validation of results.

These challenges will be discussed in the broader context of ceramic feedthru package design allowing a general understanding of the FEM and its application in package reliability.

Traditional MMIC device packages such as the one shown in Fig. 1 frequently consist of a multilayer dielectric material that electrically isolates the feedthru from the metal seal ring and heat sink components. As is typical in the manufacture of this package, screen-printed tungsten metallization and 92% alumina are cofired in a reducing atmosphere. This is followed by electrodeposition of a Ni layer which supports wetting of the 72Ag-28Cu wt% eutectic composition braze alloy. The subassembly is then high temperature brazed into a controlled expansion alloy seal ring such as a Kovar™ that is itself brazed onto a high thermal conductivity W-Cu heat sink (more commonly CuW). The explanation of the various package level components are illustrated in Fig. 2

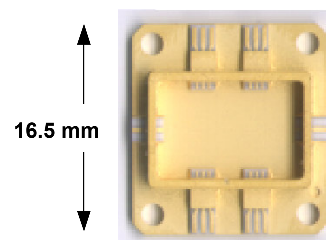

Fig. 1 Monolithic Microwave Integrated Circuit package

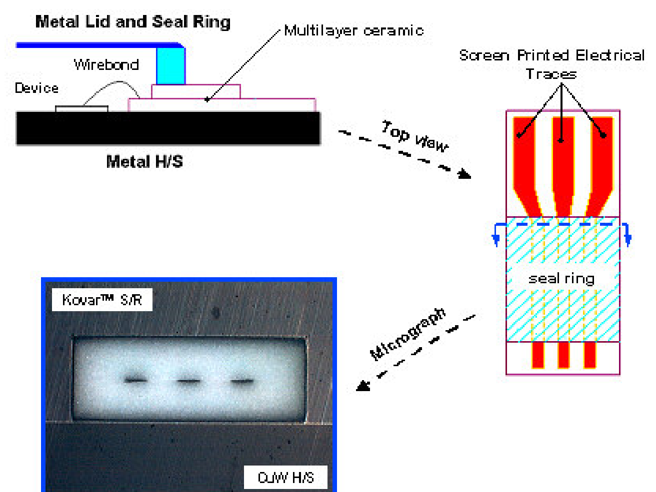

Fig. 2 MMIC package feedtru description

2.0 Material Property Characterization

Experience has shown that to *quantitatively* predict the feedthru residual stress; the FE model must incorporate the time and/or temperature dependency of both the mechanical and physical properties over the temperature range of interest.

In this case, ambient – 780°C is the temperature range that will be investigated. Clearly, a well-characterized material is fundamental, but is all of this detail necessary or warranted given today's rapid development cycles? A fundamental principal that others [2] have proposed before clarifying this is: "Understand what material behavior is *sufficient* for the analysis objective in mind." The following section provides some general guidelines in that regard.

2.1 Fe-Ni-Co (Kovar) Seal Ring. A key issue that must be addressed with any controlled expansion Fe-Ni alloy is the highly nonlinear behavior seen in the coefficient of thermal expansion (CTE) occurring past the materials Curie point [3]. As shown in Fig. 3 the seal ring material is well matched to alumina up to approx 425°C. Afterwards, the iron expansion contribution dominates causing a dramatic expansion differential with the alumina feedthru. Realizing this represents a non-conservative loading situation in the feedthru during braze solidification; detailed thermal expansion measurements ensuring enough data points to capture the transitional behavior must be included in the FE model.

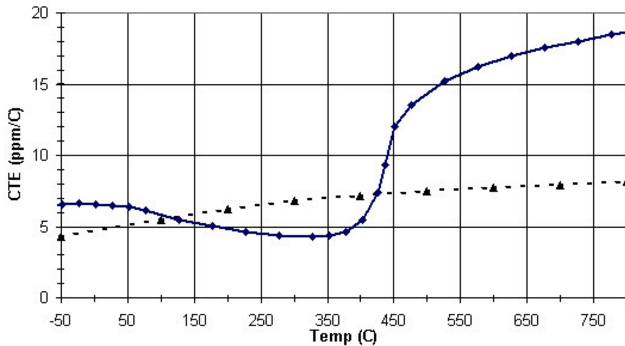

Fig. 3 Kovar, 92% Al_2O_3 Secant CTE Comparison

It should be pointed out that ANSYS software uses the secant (or mean) CTE definition instead of the tangent (or instantaneous) CTE definition used in other general purpose FE software codes [4]. The secant CTE can be defined as:

$$\alpha_s(T) \equiv \frac{1}{l_o}\frac{l - l_o}{(T - T_{ref})} = \frac{\varepsilon_{th}(T)}{T - T_{ref}} \tag{1}$$

where T_{ref} is the definition temperature about which the data is measured. It should also be noted, the definition temperature defined in Eq. (1) is also taken as the zero strain temperature for the analysis. If this is not the case, an adjustment must be made to the temperature dependent expansion data [5]. The tangent CTE can be similarly defined as:

$$\alpha_i \equiv \frac{d\varepsilon_{th}(T)}{dT} \tag{2}$$

and is independent of the reference temperature at which the data is taken. Substituting (1) into (2) and using the product rule of differentiation provides a useful relation between the two definitions.

$$\alpha_i = \alpha_s(T) + (T - T_{ref})\frac{d\alpha_s(T)}{dT} \tag{3}$$

Figure 4 graphically illustrates the different CTE definitions. A more rigorous theory treatment and error analysis can be found elsewhere [6-7].

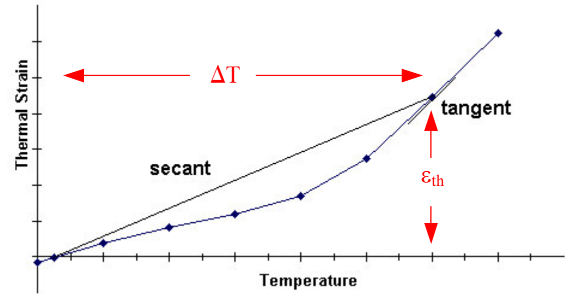

Fig. 4 Secant & Tangent CTE definitions

2.2 Eutectic Ag-Cu Braze Alloy. Residual stress generated during adhesive bonding can depend on a number of factors both material and geometrical. In the feedthru braze joint geometry considered here; the dominant loading has a strong hydrostatic stress component. Therefore, it has a limited potential for creep induced stress relaxation. Additionally, creep-induced stress relaxation would be likely if this package were processed in a batch furnace with extended cool-down times. The belt furnace used in the manufacture of this package generally does not allow sufficient time for such relaxation to occur (typically above 500°C) [8]. Therefore, considering both effects coupled with a presumed dramatic change in the mechanical behavior as the material's solidus temperature of 780°C is approached. A rate-independent constitutive plasticity theory can be assumed using a nonlinear isotropic hardening rule with an associated von Mises yield criteria. The choice of hardening rule describes the changing of the yield surface with progressive plastic strain, so that the conditions for subsequent straining can be established. In this case, an isotropic hardening condition can be chosen due to the absence of cyclic loading conditions (e.g. Bauschinger effect) [9]. This nonlinear hardening option NLISO within ANSYS is a variation of the classic P. Ludwik empirical model (1909) where an exponential saturation hardening term is appended to the linear term. The advantage of this model is the material behavior is defined in terms of a function having four material constants that can be determined from true stress-plastic strain curve fitting. Thus, allowing a smooth transition into the plastic tangent modulus.

$$\sigma = \mathbf{k} + \mathbf{R}_o\varepsilon_p + \mathbf{R}_\infty\left[1 - \frac{1}{e^{\mathbf{b}\varepsilon_p}}\right] \tag{4}$$

The constants for Eq. (4) were determined using a nonlinear regression algorithm fit to seven experimentally measured braze plasticity curves. The results of this data reduction are

shown in Fig. 5. It should be acknowledged that all raw braze plasticity and elastic modulus data was made available through the Materials Joining department at Sandia National Laboratories [10]. The details of the material preparation and mechanical testing methods for this data can be found in references [11-12].

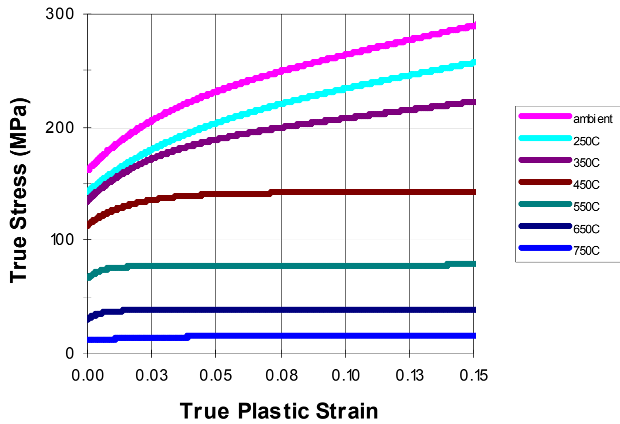

Fig. 5 True stress-strain curves for Silver-Copper braze alloy

2.3 W-Cu Dispersed Composite Heat Sink. Not expanded on here for brevity, but of equal importance, is the temperature dependency behavior seen in the thermophysical properties of these materials. The properties of these composites will also be a function of the constituent material weight percentages used in manufacture and will strongly influence the final camber of the package. Therefore, these material sets warrant a careful characterization of their properties over temperature.

***NOTE**: The afore mentioned discussion is intended to only give general insight into the level of material characterization required for this type of stress analysis and should not be considered all inclusive.*

3.0 Finite Element Model

In the present work, a 3D isothermal rate-independent finite element model was created using ANSYS release 7.1. In order to keep computation time at a minimum, ¼ symmetry was exploited in the analysis. As shown in Fig. 6, the mesh is composed of linear "brick" elements that have been extruded into the *z* coordinate direction from an in-plane representation. This method ensures a robust element for numerical stability and a minimum amount of degrees-of-freedom to be computationally solved for. The simulation methodology implemented consists of a sequential isothermal "ramp-up" and then "cool-down" load step approach (e.g. ambient→780°C then 780°C→ambient). In the ramp-up load step, all braze layers are deactivated from the analysis via multiplying their elemental stiffness by a small constant term. This "birth-death" technique correctly models the actual manufacturing situation where all stacked components are not rigidly attached prior to brazing. In the cool-down load step, the braze layers are reactivated and assigned a new zero strain temperature of 780°C. All other materials retain their original zero strain temperature of ambient. This change ensures no residual strain will be present in the braze during the start of cool-down [13]. The assembly is then allowed to isothermally cool-down to the prescribed ambient temperature. The isothermal approximation can be realized if one considers the relatively high thermal diffusivity and small size of all package level components.

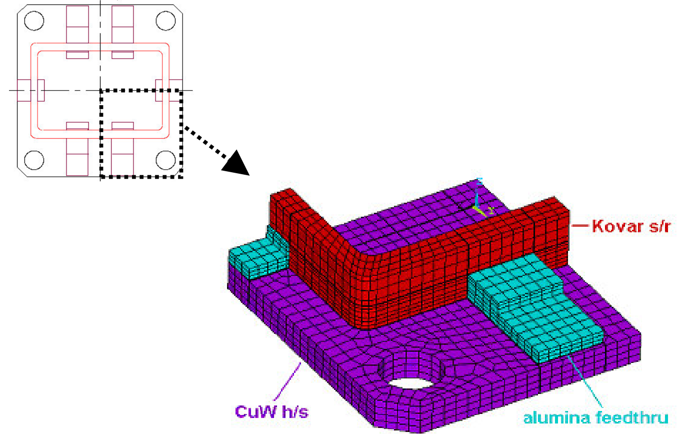

Fig. 6 MMIC package finite element model

3.1 Fine detail stress resolution via submodeling technique. In the stress analysis of this package, a nonlinear global model with a relatively course mesh provided insight into the vulnerable feedthru region for the subsequent local submodel analysis (Fig. 7). This well know technique for resolving such fine detail stress gradients is absolutely necessary in microelectronic package design given the large variation in critical feature length scales. Submodeling is also known as the cut-boundary displacement method. The cut-boundary is the boundary of the submodel, which represents a slice through the global model. Displacements calculated on the cut boundary of the global model are specified as boundary conditions for the submodel. Submodeling is based on Saint Venant's principle, which in classical mechanics implies that stress concentration effects are very localized. Therefore, if the boundaries of the submodel are far enough away from the stress concentration, accurate results can be assumed for the submodel.

An additional consideration mentioned previously, is the non-conservative loading situation encountered in this analysis (e.g. calculated displacements are load path dependent). Realizing the global model cut-boundary displacements, when applied to the submodel, will be linearly interpolated for each load step; sufficient detail must be included in the submodel load steps from the global model solution to capture these effects. In this analysis a minimum of eight load steps during braze cool-down was determined as sufficient.

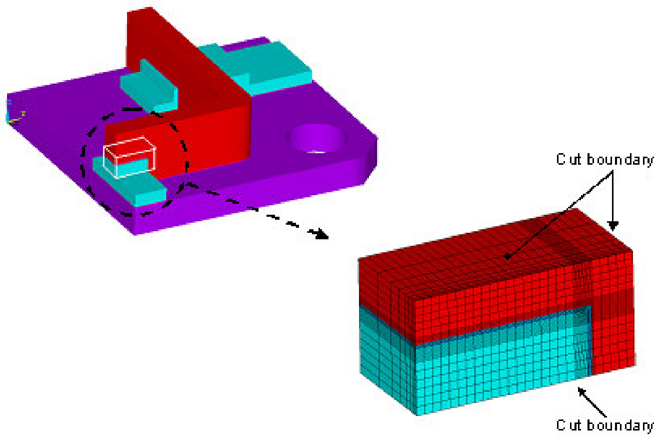

Fig. 7 Global finite element model shown left, with critical region local model shown right

4.0 Statistical Nature of Failure in Brittle Materials

Ceramic brittle fracture is the dominant failure mode observed in microelectronics. This fast fracture is governed by random strength limiting flaws (approx. 5-200μm) leading to the observed statistical nature of component failure seen in practice. It is therefore vital that any ceramic package design include a probabilistic design methodology for predicting this material failure response. Understanding this challenge, the Structural Integrity Branch at the NASA Lewis Research Center has developed CARES/*Life* design software (Ceramics Analysis and Reliability Evaluation of Structures) [14]. This modular software program can be coupled with most commercial finite element codes allowing a departure from the traditional deterministic modeling approach to a more appropriate statistical design based approach (Fig. 8).

The probabilistic design approach developed here involves determining the statistical failure probability for a thermomechanically stressed monolithic ceramic component based on simple test geometry fast fracture data. This approach differs greatly from the failure criteria utilized in ductile materials (e.g. metals). In ductile materials the high local stresses are able to redistribute locally through inelastic deformation mitigating any apparent distribution in ultimate strength values. Typically, a four-point flexural test is conducted in order to characterize the cumulative failure distribution of the material under study (refer ASTM C1160-90). In this work a more conservative two parameter Weibull distribution was fit to the data instead of the three parameter formulation. Figure 9 shows a typical fractographically labeled Weibull plot for sintered alumina under conditions of three-point flexure [15]. It should also be mentioned that extrapolation of simple test fracture strength data to complicated geometry works best when the test specimen corresponds to the component in size, stress state, and defect distribution. Stated another way, strength is *not* an intrinsic property of a brittle material.

For this analysis, the required input for the CARES/*Life* software included proprietary measured three-point flexure data, along with finite element submodel stresses via ASCII character neutral file. This data was then used to determine the reliability of each finite element sub-volume at the Gaussian integration points assuming randomly distributed volume flaws control the failure response. The probability of survival for each element is therefore considered mutually exclusive, and the overall component reliability is then the summation of all the survival probabilities. Extending this failure criterion to a more general multiaxial stress state condition, the Principal of Independent Action (PIA) phenomenological model was chosen, primarily because of its simplicity. The PIA theory assumes that each tensile principal stress contributes to the failure probability as if no other stress were present. Thus, the sub-volume probability of failure can be expressed by the following:

$$P_{f_V} = 1 - \exp\left[-\int_V \left(\left(\frac{\sigma_1}{\beta_o}\right)^{m_V} + \left(\frac{\sigma_2}{\beta_o}\right)^{m_V} + \left(\frac{\sigma_3}{\beta_o}\right)^{m_V} \right) dV \right] \quad (5)$$

where the Weibull scale parameter, β_o represents a unit volume characteristic strength in which $[1\text{-}e^{-1}]$ percent of the test specimens have failed. The degree of scatter of the fracture strength data is characterized by the modulus m_v (approx. 5-15 in ceramics). $\sigma_{1\text{-}3}$ is the principal stress component evaluated by the finite element software.

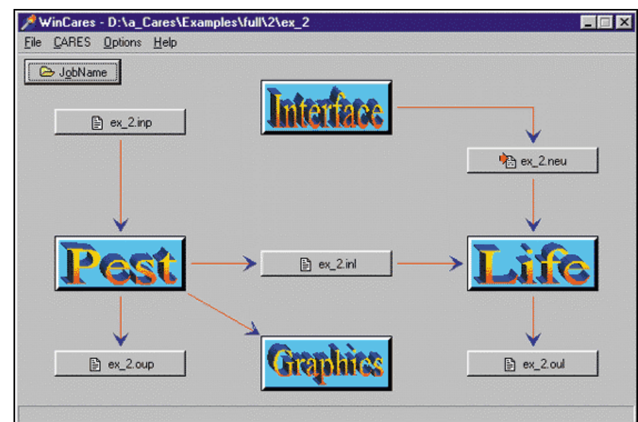

(a)

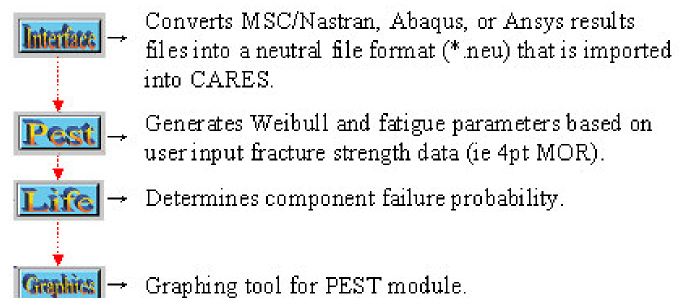

(b)

Fig. 8 CARES/*Life* design software: (a) program GUI, (b) descriptions of the four modular programs

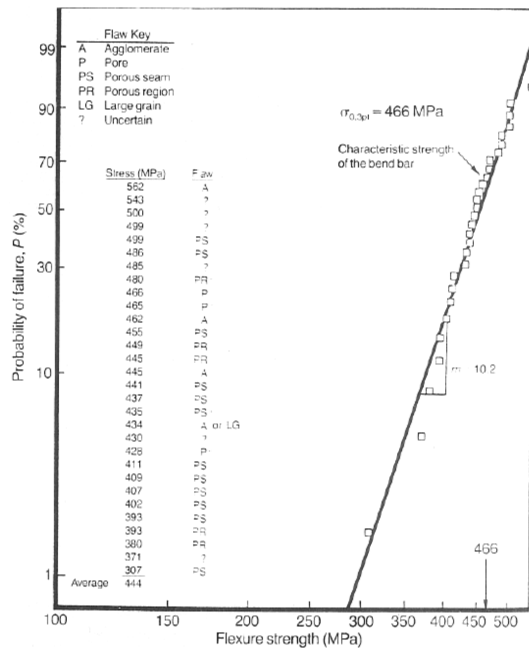

Fig. 9 Fractographically labeled Weibull failure plot for Al_2O_3 under conditions of 3-pt flexure, ASTM size B specimen (from Ref. 15)

5.0 Design Application

Recalling the original design objective is to minimize the thermomechanical residual stresses in the ceramic feedthru or conversely improve the package reliability. The initial design was simulated and the first principle stress contour plots are shown in Fig. 10. It is seen that these results match the failure mode and location seen in practice. While not detailed here in an additional plot, the overall feedthru failure probability was .86% with the maximum sub-volume failure probability corresponding to the peak finite element principal stress location. Also shown in Fig. 10a is the assumed inverse distance law effect in which the tensile stress at the braze/alumina interface is high enough to cause subcritical crack initiation (e.g. regime I in crack velocity vs. K_I graph). The magnitude drops off extremely rapidly causing this subcritical crack growth to be halted as the applied stress in lowered below the critical stress intensity factor K_{IC}.

Additionally, since this package represents a legacy product outline, only limited design changes could be realized. Therefore, different compositional W-Cu heat sinks were simulated with a significant improvement in reliability being determined as tungsten content was increased. Of course, the thermal penalty due to decreased heat sink conductivity must be weighted against the presumed increased package reliability. While not appropriate here, a design iteration involving finding the optimal heat sink thickness showed additional reliability improvements for this package style.

5.1 FE Model Validation. The rationale for model validation in this work was based on the premise that the finite element stress field involves partial differentiation of the nodal displacement shape function. Hence, the global model correlation to experimental deflection data can be considered a 2nd order validation of the finite element submodel stress field. Other more direct 1st order methods like moire´ interferometry are preferred. In this case, a total of fifteen randomly selected packages were measured for pre and post-braze deflection. It was observed that the FE global model correlated to within 20% of the experimental anticlastic deflection values. The measured deflection plot also *qualitatively* matched the general shape of the heat sink plot shown in Fig 11.

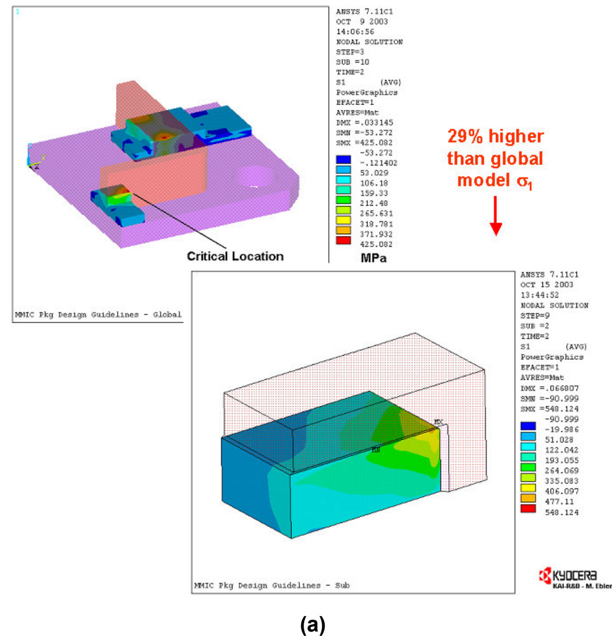

(a)

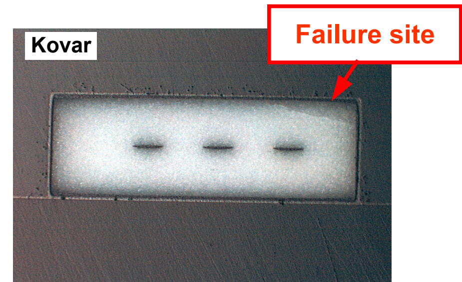

Fig. 10 (a) FE global/local model first principal stress contour plot (in MPa), (b) micrograph showing typical feedthru failure

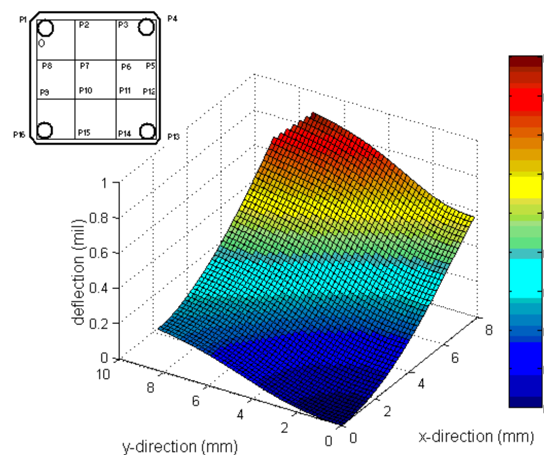

Fig. 11 MMIC package heat sink measurement locations shown left, ¼ finite element model anticlastic deformation plot shown right

6.0 Conclusions

As this work seeks to demonstrate, the thermomechanical response of ceramic feedthru packages can be effectively modeled without the need for any product dependent calibration factors using standard finite element tools coupled with a probabilistic design strategy. Hence, establishing an *absolute* methodology for the development of future high reliability microelectronic ceramic feedthru packages within our organization.

Acknowledgments

The author wishes to thank our multilayer manufacturing division management for providing support and encouragement during this project. Thanks are also extended to our analytical laboratory personnel for the excellent micrographs contained in this report.

References

1. Saito, R., Griese, J., Kessler, J., Kono, R., Fang, J., "Hydrogen Degradation of GaAs MMICs and Hydrogen Evolution in the Hermetic Package," IEEE 1995 Microwave and Millimeter-Wave Monolithic Circuits Symposium, Orlando, FL, May. 1995.

2. Syed, Ahmer, "Predicting Solder Joint Reliability for Thermal, Power, & Bend Cycle within 25% Accuracy," *Proc 51th Electronic Components and Technology Conf.*, Orlando, FL, May. 2000, pp. 255-263.

3. Harner, Lesile L., "Selecting Controlled Expansion Alloys," *Carpenter Technology Corporation On-line Technical Articles*, http://crswnew.cartech.com/wnew/techarticles/TA00011.html, August. 1994, pp. 255-263.

4. MSC MARC 2001 Volume A: Theory and User Information, MSC Software Corp., Redwood City , CA.

5. ANSYS Theory Reference Manual, Release 7.1, ANSYS Inc., Canonsburg, PA.

6. Pao, Yi-Hsin., Jih, Edwards., Artz, Bruce E., "A Note on the Implementation of Temperature Dependent Coefficient of Thermal Expansion (CTE) in ABAQUS," *ASME Trans-Journal of Electronic Packaging*, Vol. 114, (1992), pp. 470-472.

7. Touloukin, Y.S., Kirby, R.K., Taylor, R.E., Lee, T.R., Thermophysical Properties of Matter, Vol. 12 Thermal Expansion: Metallic Elements and Alloys, IFI/Plenum (New York, 1977), pp. 17a-25a.

8. Romig, A.D., Frear, D.R., Hlava, P.F., Hosking, F.M., Stephens J.J., Vianco, P.T., "Microstructural Characterization of Solders and Brazes for Advanced Packaging Technology," Report SAND91-0698C, Sandia National Laboratories, Albuquerque, NM.

9. Mendelson, Alexander., Plasticity: Theory and Applications, Krieger Publishing Company (Florida, 1983), pp. 13-20.

10. Stephens, John J., personal communication, 1999.

11. Neilsen, M.K., Stephens J.J., Gieske, J.H., "A Viscoplastic Model For The Eutectic Silver-Copper Braze Alloy," *ASM/AWS 2nd International Brazing & Soldering Conference*, San Diego, CA, Feb. 2003.

12. Stephens J.J., Burchett, S.N., Jones, W.B., "Stress Relaxation of Braze Joints," Report SAND92-0190C, Sandia National Laboratories, Albuquerque, NM.

13. Deibel, Farrell L., "Calculating Residual Manufacturing Stresses in Braze Joints Using ANSYS," *IEEE Trans-Electronic Devices*, Vol. 34, No. 5, (1987), pp. 1214-1217.

14. Nemeth, N.N., Janosik, L.A., Palko, J.L., "CARES/*Life* Software For Characterizing And Predicting The Lifetime of Ceramic Parts," *Proc. NAFEMS World Congress*, Newport, RI, May. 1999.

15. Quinn, George D., Morrell Roger., "Design Data for Engineering Ceramics: A Review of the Flexure Test," *Journal of America Ceramic Society*, Vol. 74, No. 9 (1991), pp. 2037-2066.